Hardness and Chemical Potential Profiles for Some Open-Shell HAB → HBA Type Reactions. Ab Initio and Density Functional Study

Tapas Kar and Steve Scheiner

Department of Chemistry, Southern Illinois University, Carbondale, Illinois 62901

A. B. Sannigrahi*

Department of Chemistry, Indian Institute of Technology, Kharagpur-721 302, India

Received: February 3, 1998; In Final Form: April 24, 1998

The electronic structure, hardness (η), and chemical potential (μ) for the ^{1}A′ and ^{3}A″ states of HNO−HON and the ^{2}A″ state of HSO−HOS have been calculated using HF/6-311++G** and B3LYP/6-311++G** methods. The η and μ profiles of the ^{1}A′ state of HNO−HON and those of HSO−HOS are obtained in agreement with the salient features of the maximum hardness principle (MHP). However, a quite erratic η profile is predicted for the ^{3}A″ state of HNO−HON. This can be attributed to the nature of the variation in the energy difference of the two states along the reaction path. The relative energies, ionization potentials (I), and electron affinities (A) are calculated at the stationary points of the B3LYP surface using B3LYP and MPn (Full) methods. Most of these values are obtained in very good agreement with the available experimental data. The η values based on these I and A identify the most stable species correctly but do not follow the expected trend with regard to the relative stability of the transition state. The reason for this anomaly is discussed.

1. Introduction

The concept of hardness was first introduced by Mulliken[1] and Pearson.[2] It has now been established as a very useful concept in the theory of electronic structure and reactivity of molecules. In the framework of the density functional theory (DFT),[3] hardness (η) is related[4] to the slope of the μ vs N curve (μ is the chemical potential[5] and N is the number of electrons) at constant external potential and temperature. The chemical potential was defined earlier.[5] It is equal to the slope of the E vs N curve, where E is the total energy. Thus, η is related to the curvature of the E vs N curve. Using three-point finite difference approximation for the energy derivatives, Pearson[6] derived the following working expressions for η and μ.

$$\eta = (I - A)/2 \tag{1}$$

$$\mu = -(I + A)/2 \tag{2}$$

where I and A are respectively the ionization potential and electron affinity of the N-electron system. For closed-shell systems eqs 1 and 2 can be further simplified by using Koopmans' approximation (KA) for I and A.

On the basis of empirical observations, Pearson[7] proposed a very important principle of molecular electronic structure, which is now known as the maximum hardness principle (MHP). It has evoked considerable research activity in this area, culminating in a large number of papers[8−18] published in quick succession. In these studies η and μ have been calculated for a variety of individual molecules, for structural changes in molecules caused by inversion, deformation, internal rotation, etc., and for various types of simple reactions. The main conclusions of these studies are as follows: (1) A more stable structure is usually associated with a higher value of η and a lower value of μ. (2) Exothermic reactions are accompanied by an increase in η. (3) The computed hardness profiles (change of η along a reaction path) pass through a minimum at or near the transition state (TS) for internal rotation, inversion, exchange, and isomerization types of reactions.

We are concerned here with the isomerization reactions of the type HAB → ABH, which are brought about by a 1,2-hydrogen shift. The first reaction of this kind for which the η and μ profiles were calculated[16] is the isomerization of HCP to HPC. Kar and Scheiner[17] calculated the η and μ profiles of a number of 10-valence electron closed-shell HAB−HBA systems derived from first- and second-row elements. They used KA to evaluate I and A and observed that hardness is a good indicator of the more stable isomer. An important finding of this study is that while the total energy does not exhibit the same behavior as η and μ, the individual electronic (E_{el}) and nuclear repulsion (V_{nn}) energies are in close parallel with them in most cases. This is in agreement with the proposition[8] made on the basis of theoretical arguments.

Density functional calculations of hardness, electronegativity (χ, the negative of μ), and polarizability for a number of similar systems have recently been reported by Ghanty and Ghosh.[17] Some of the molecules chosen by them contain third-row elements as well. Following KA, the energies of the highest occupied and lowest unoccupied Kohn−Sham (KS) orbitals[19] were used to calculate I and A. They did not calculate the η and μ profiles, and the geometries of HAB, HBA, and BHA (TS) were taken from the literature. The TS in most cases was found to be associated with a minimum value of η and a maximum value of μ. There are, however, a number of exceptions in the ordering of η and μ vis-à-vis that of total energy.

In the present investigation we have extended the works of Kar and Scheiner[17] and of Ghanty and Ghosh[17] to open-shell

S1089-5639(98)00988-8 CCC: $15.00
Published on Web 06/26/1998

systems for which only a few calculations have so far been reported.[18] The specific systems we have chosen here are HNO−HON and HSO−HOS. These molecules play a very important role in atmospheric chemistry. For the former we have considered ^{1}A′ and ^{3}A″ states, and for the latter the ^{2}A″ state has been taken into account. Hardness and chemical potential have been calculated using HF (UHF for open-shell species) and the B3LYP (Becke[20] three-parameter nonlocal exchange functional with the nonlocal correlation functional of Lee, Yang, and Parr[21]) method. Although somewhat semiempirical in nature, the B3LYP method has been found[22] to be quite reliable in the study of electronic structure and energetics of a wide variety of molecules. The present study is probably the first application of B3LYP or any other version of the density functional method in the calculation of η and μ profiles of open-shell systems. Since Koopmans' approximation cannot be used unambiguously for a UHF wave function, we have calculated I and A for the open-shell molecules by the energy difference (ΔE) method, where separate calculations are carried out for the neutral species and its ions. Finally, single-point MP2 and MP4SDTQ calculations are performed at the stationary points of the B3LYP potential energy (PE) surface. The η and μ values obtained thereby are then compared with the B3LYP values.

2. Method of Computation

All calculations have been carried out using the Gaussion-94 program.[23] The 6-311++G** basis set has been used in both HF and DF (this shorter acronym denoting density functional has often been used here for B3LYP) methods. All electrons are correlated in the single-point MPn calculations which are of RMPn type for the closed-shell and of UMPn type for the open-shell systems. Since the energies in the UMPn calculations are generally overestimated due to spin contamination in the reference UHF wave function, we have used projected UMPn or PUMPn method.

3. Results and Discussion

Although our primary objective is to study the nature of η and μ profiles, we have given due emphasis to the equilibrium structure and energetics in order to assess the overall performance of the B3LYP method. In what follows geometries, relative energies of the neutral species, the η and μ profiles, and the values of η and μ at the stationary points in the PE surface are presented in separate subsections.

A. Geometries. The HF and B3LYP optimized geometries for HNO−HON and their ions are summarized in Table 1. Available experimental values and results of some previous calculations[24,25] carried out at different levels of electron correlation treatment (MP2/Full/6-311G** and CASSCF) are also included in this table for the sake of comparison. As is well-known, the HF method fails to predict the correct ground state for HNO. For the present systems the NO bond length is underestimated by this method. The best overall agreement with experiment is achieved by the CASSCF calculations.[25] The performance of MP2 and B3LYP methods is comparable; in most cases they yield results in good agreement with experiment. Barring the bond angle in the ^{3}A″ state of HNO which is highly exaggerated by the MP2 method and by about 5° in the B3LYP method, the geometries predicted by the correlated methods vary within a small range. The geometries for some of the systems obtained by Mebel et al.[26] using the B3LYP/6-311 g(d,p) method are found to be virtually identical to the corresponding values derived here using a slightly higher basis set. For the ions the geometries have been optimized only by the B3LYP method. Unfortunately, no experimental values are available for comparison.

TABLE 1: Optimized Geometries (Bond Length in Å and Bond Angle in deg) of the HNO−HON System and Its Ions

system XYZ	distance XY	distance YZ	angle XYZ	method[a]
HNO(^{1}A′)	1.032	1.167	109.4	A
	1.064	1.200	108.9	B
	1.053	1.220	107.6	C
	1.053	1.217	107.8	D
	1.064	1.212	108.8	exptl
HNO(^{3}A″)	1.013	1.219	113.7	A
	1.021	1.224	119.8	B
	1.024	1.200	127.4	C
	1.011	1.238	117.0	D
	1.021	1.238	114.6	exptl
HON(^{1}A′)	0.967	1.240	111.4	A
	1.001	1.254	112.7	B
	0.985	1.256	110.3	C
	1.005	1.270	111.2	D
	0.984	1.286	111.0	exptl
HON(^{3}A″)	0.948	1.310	109.1	A
	0.970	1.324	109.5	B
	0.967	1.322	106.5	C
	0.984	1.323	110.0	D
	0.974	1.344	107.2	exptl
OHN(^{1}A′)	1.004	1.200	66.4	A
	1.109	1.266	67.6	B
	1.017	1.287	67.6	C
	1.090	1.275	68.4	D
OHN(^{3}A″)	1.196	1.202	65.1	A
	1.185	1.228	66.8	B
	1.179	1.173	67.8	C
	1.151	1.233	68.4	D
HNO^+(^{2}A″)	1.079	1.223	124.2	B
HON^+(^{2}A″)	1.026	1.173	118.8	B
HNO^-(^{2}A″)	1.060	1.328	106.5	B
HON^-(^{2}A″)	0.965	1.465	104.9	B

[a] Entries against A (HF/6-311++G**) and B (B3LYP/6-311++G**) refer to this work. Methods C (ref 24) and D (ref 25) stand for MP2(Full)/6-311G** and CASSCF, respectively. Experimental values are quoted in ref 25.

The optimized geometries of HSO−SOH and its ions are compared in Table 2 with the results of some earlier calculations.[27−31] The experimental geometry[32] is available only for HSO. As in the HNO−HON system, the HF bond lengths are appreciably underestimated. For the HSO radical the closest correspondence with experiment[32] is obtained by the MP2 method. The B3LYP and MP2 geometries of HSO−HOS differ by a somewhat greater margin than in HNO−HON. This difference is most pronounced in the TS (OHS) for which the MRDCI (multireference double excitation configuration interaction) results[28] fall well outside the range of the present values. This discrepancy is possibly due to the inefficient (curve fitting using insufficient number of points) optimization procedure[28] used for OHS in the MRDCI calculations. The HF method predicts a wrong ground state for the HSO^+ ion which is isoelectronic with HNO. Comparable geometries are predicted for the ions by the B3LYP and MRDCI methods.

B. Relative Energies of the Neutral Species. The relative energies (E_{rel}) of the neutral species as obtained by PUMP2-(Full), PUMP4SDTQ(Full), and B3LYP methods at the stationary points of the B3LYP PE surface are given in Table 3 along with the results of some earlier high-level ab initio calculations.[24,25,30] The ZPE (zero point energy) corrections are included in the relative energies. In this work (A, B, and C,

TABLE 2: Optimized Geometries (Bond Length in Å and Bond Angle in deg) of the HSO−HOS System and Its Ions

system XYZ	state	distance XY	distance YZ	angle XYZ	method[a]
HSO(^{2}A″)		1.341	1.535	101.5	A
		1.380	1.533	103.9	B
		1.368	1.490	106.6	C
		1.367	1.557	101.3	D
		1.392	1.519	104.1	E
		1.389	1.494	106.6	exptl
HOS(^{2}A″)		0.944	1.619	111.2	A
		0.968	1.662	109.1	B
		0.977	1.654	107.7	C
		0.950	1.625	109.8	D
		0.952	1.646	109.5	E
OHS(^{2}A″)		1.301	1.422	72.7	A
		1.355	1.438	74.1	B
		1.402	1.397	67.8	C
		1.135	1.514	80.8	E
HSO^+(^{1}A′)		1.362	1.409	103.8	A
		1.397	1.455	103.8	B
		1.371	1.482	104.5	C
		1.365	1.466	104.8	E
HSO^+(3A″)		1.353	1.550	94.6	A
		1.392	1.554	95.2	B
		1.364	1.568	92.7	C
		1.365	1.561	97.8	E
HOS^+(^{1}A′)		0.964	1.501	118.2	A
		0.974	1.550	116.3	B
		0.977	1.579	118.3	E
HOS^+(^{3}A″)		0.961	1.579	123.4	A
		0.965	1.554	124.3	B
		0.979	1.529	124.4	E
HSO^-(^{1}A′)		1.355	1.585	105.1	A
		1.393	1.616	106.4	B
		1.349	1.593	105.9	E
HOS^-(^{1}A′)		0.938	1.756	105.4	A
		0.960	1.831	102.1	B
		0.953	1.773	104.3	E

[a] Entries against A (HF/6-311++G**) and B (B3LYP/6-311++G**) refer to this work. Methods C (ref. 30), D (ref. 27) and E (ref. 29) stand for MP2(Full)/6-311G** MCSCF, and MRDCI, respectively.

TABLE 3: Relative Energies (E_{rel}, kcal/mol) of HNO−HON and HSO−HOS Systems

system	state	E_{rel}[a] A	B	C	D	E	F	G
HNO	^{1}A′	0.0	0.0	0.0	0.0	0.0		
	^{3}A″	20.7	20.9	11.0	21.1	18.4		
HON	^{1}A′	48.5	45.3	40.7	45.9	42.6		
	^{3}A″	25.1	24.9	20.4	25.4	23.2		
OHN	^{3}A″	73.7	70.0	72.9	70.5	72.5		
	^{3}A″	57.9	56.8	53.2	57.1	58.8		
HSO	^{2}A″	0.0	0.0	0.0			0.0	0.0
HOS	^{2}A″	−7.6	−4.3	−1.4			−4.8	3.4
OHS	^{2}A″	53.8	53.7	44.0			47.0	46.0

[a] Values under A (PUMP2(Full)/X//Y/X), B (PUMP4SDTQ(Full)/X//Y/X), and C (Y/X//Y/X) are from this work, where X = 6-311++G** and Y = B3LYP. Values under D (ref 24), E (ref 25), F (ref 30), and G (ref 30) correspond respectively to PUMP4SDTQ(Full)/6-3111G**//MP2(Full)/6-311G**, CASSCF, MP4/6-311G(d, p)//MP2 (Full)/6-31G(d), and G-2//MP2(Full)/6-31G(d) calculations.

see Table 3), ZPE's of ref 24 are used for HNO−HON and those of ref 30 are used for HSO−HOS. For the singlet states, RMPn calculations have been performed throughout. The relative energy of the ^{3}A″ state of HNO and the barrier height in the ^{3}A″ surface of HNO−HON seem to be somewhat underestimated in the B3LYP calculations, which otherwise yield results in good agreement with the CASSCF values. Although slightly different basis sets and geometries have been employed in the two sets of PUMP4 calculation, they predict practically identical values for relative energies.

Ab initio calculations for the HSO and SOH radicals were first reported by Sannigrahi et al.[33] They predicted HOS to be more stable than HSO. Several ab initio calculations[34] reported thereafter made an identical prediction although the magnitude of the energy difference was found to decrease with the improvement in the quality of calculations. It was pointed out by Xantheas and Dunning[35] that failure to account for dynamic correlation, inadequacy of the basis sets, and poor geometries were the main reasons why earlier calculations failed to correctly predict the relative stability of HSO and HOS. It has now been firmly established[30] that HSO is more stable than HOS. As can be seen from Table 3, the B3LYP method fails to predict the correct sign of E_{rel}, although the magnitude of E_{rel} is quite small. The best estimate for this quantity has been obtained[30] using the Gaussian-2 theory.[36] The G-2 and B3LYP barrier heights are virtually identical. This agreement is likely fortuitous: the errors in energies seem to have been canceled out due to the use of somewhat different geometries.

C. Hardness and Chemical Potential Profiles. In the preceding subsections we have seen that the B3LYP method yields equilibrium structures for the neutral as well as ionic species and the energetics of the neutral species in good agreement with the results of earlier calculations and experimental data, where available. We will now compare the η and μ profiles obtained by B3LYP and HF methods.

The reaction path for the isomerization of HAB to HBA is conveniently[17] described by the variation of the HAB angle (θ). Along this reaction path η and μ values are calculated by the ΔE method using the vertical values of I and A. For the ^{1}A′ state of HNO−HON Koopmans' approximation has also been used. The η profiles thus calculated using B3LYP method are displayed along with the energy values in Figure 1a, and the corresponding HF results are given in Figure 1b.

As can be seen from Figure 1a, the ^{3}A″ state of HON (where $\theta = 30°$) is lower in energy than the ^{1}A′ state of HON, and in the case of HNO (where $\theta \approx 110°$) the order is reversed. The transition state ($\theta = 55°$) of the ^{3}A″ surface, is found to be lower than the ^{1}A′ surface, and the two surfaces cross at $\theta = 73°$. These findings are in accordance with the previously reported results.[24,25] It may be noted that these trends in energy profiles are not correctly predicted by the HF method (see Figure 1b). The ^{3}A″ state of HON is found (Figure 1b) to be the global minimum in the surface—which is certainly not the case.

We first discuss the nature of the η profiles of the ^{1}A′ surface of HNO−HON drawn in Figure 1a. The KA η profile is characterized by two maxima ($\theta = 30°$ and 105°) and a minimum ($\theta = 45°$). They refer to HON, HNO, and OHN (transition state), respectively, and occur at or near the corresponding points in the E profile. The behavior of the η profile (^{1}A′ surface) calculated by the ΔE method follows the same trend and contains extrema at the same HNO angles. The only difference between these two η profiles is the magnitude of the η values, i.e., η(KA) (1−2 eV) $\ll$ $\eta(\Delta E)$ (5−6 eV). This is due to the fact that energies of the occupied (unoccupied) KS orbitals are markedly higher (lower) than the corresponding HF orbital energies. Because of the orbital energy difference, the Koopmans' I values are underestimated and A values are overestimated in the B3LYP method. The nature of the μ profile (not shown) of the ^{1}A′ surface closely follows that of the hardness, only in reverse: the minima of μ occur at points which are maxima for η. These trends also hold for the HF approximation except the KA method where the maximum at

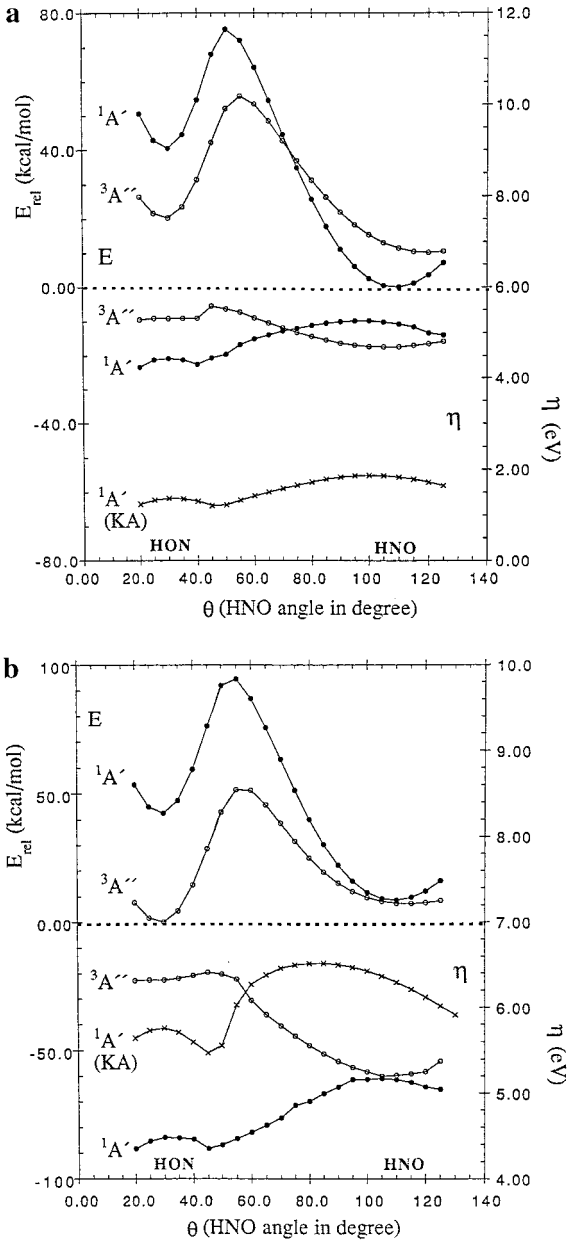

Figure 1. (a) Plots of relative energies (E_{rel}, left scale) and hardness (η) obtained by DFT method of HNO against HNO angle (θ). (b) Plots of relative energies (E_{rel}, left scale) and hardness (η) obtained by HF method of HNO against HNO angle (θ).

$\theta = 80°$ does not refer to any stationary point in the E profile. At the stationary points of the η and μ profiles the following relations hold: η(HNO) > η(HON) > η(TS) and μ(HNO) < μ(HON) < μ(TS). This is in conformity with MHP and earlier observations.[17]

According to Parr and Gazquez,[8] η should reach an extremum at a point where both electronic (E_{el}) and nuclear repulsion energy (V_{nn}) are extrema. It was further shown that when μ is constant η is a maximum at a point where E_{el} is a minimum, and vice versa. The same conclusion is valid when μ is not constant, but it has an extremum at the same point where E_{el} does. For the discussion of the nature of these profiles it is thus necessary to have knowledge of the positions of extrema in the V_{nn} and E_{el} profiles also. Figure 2 illustrates the behavior of these two components of the total energy calculated using the B3LYP method, again as a function of HNO angle. The extrema ($\theta = 35°$, 55°, and 120°) in these profiles were found

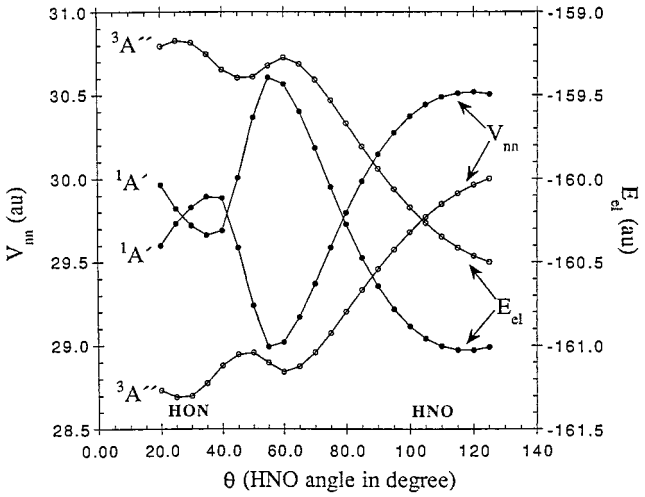

Figure 2. Variation of nuclear repulsion energy (V_{nn}, left scale) and electronic energy (E_{el}) obtained by DFT method of HNO with HNO angle (θ).

to be coincident in most cases: V_{nn} is a maximum at a point where E_{el} is a minimum, and vice versa. In fact, they are nearly perfect mirrors of one another. Kar and Scheiner[17] observed that the extrema in the η or μ profile are more tightly connected to the V_{nn} and E_{el} profiles than to their sum. Although there are slight differences in the position of the extrema, there remains a strong similarity in shape of the profiles in ^{1}A′ state of HNO−HON. In the case of μ profiles (not shown) this coincidence is rather poor.

Let us now turn our attention to the nature of the η profiles presented in parts a (B3LYP method) and b (HF method) of Figure 1 for the ^{3}A″ surface of HNO−HON. The energy difference (ΔE) method is used to calculate η and μ. As can be seen from Figure 1a,b, the nature of the profiles is quite erratic (the same is true for the μ profiles[37] which are not shown here). Some of the extrema match with the corresponding energy profiles; however, the nature of each stationary point is just the opposite to what is expected—hardness is minimum for the minimum-energy structures and maximum for the TS. This anomalous behavior can be qualitatively explained as follows. The hardness values of the two states bear the following relation.

$$\eta_3 = \eta_1 + E_1 - E_3 = \eta_1 + \Delta E_{ex} \qquad (3)$$

where 1 and 3 refer to ^{1}A′ and ^{3}A″ states, respectively, and ΔE_{ex} is the excitation energy of the ^{3}A″ state. It can be seen from Figure 1a that η_1 is a slowly varying function of θ(HNO), while ΔE_{ex} (not explicitly shown) changes much faster. Thus, it is the latter variation which determines the shape of the η_3 profile. The presence of a maximum near the TS of the ^{3}A″ state is due to the very high value of ΔE_{ex} at that point. Beyond the crossing point at $\theta = 73°$, the status of the two states is interchanged and $\Delta E_{ex} < 0$. This causes a decrease in η_3 and one gets a minimum in the η_3 profile at $\theta \approx 110°$ (here ΔE_{ex} is minimum) which corresponds to the bond angle of HNO in the ^{3}A″ state. A qualitative correlation between $\Delta\eta$ and the barrier to internal rotation has been reported.[16] A linear relationship between these two quantities has also been found in the present investigation.

We turn now to the energy and η profiles of the ^{2}A″ state of HSO−HOS system exhibited in Figure 3. Only the energy difference (ΔE) method is used to calculate η and μ. For the sake of clarity, each point in the E(HF) curve is lowered by 1 au. Both B3LYP and HF energy curves show fairly good

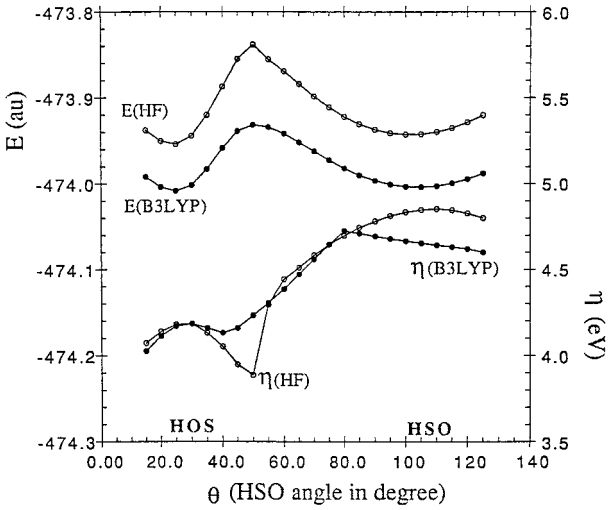

Figure 3. Dependence of total energies (E, left scale) and hardness (η) obtained by DFT and HF methods of HSO upon HSO angle (θ).

correspondence with regard to the stationary points: minima at 25° and ≈100° and a maximum at 50° correspond to HOS, HSO, and OHS (transition state). Some of these points are common to η profiles. The nature of these profiles is qualitatively similar for the HF and DF methods. In both cases the η profile is characterized by two maxima and a minimum (while the μ profiles, not shown here, exhibit some additional extrema). At the respective stationary points the following relations are satisfied by η and μ: η(HSO) > η(HOS) > η(OHS) and μ(HSO < μ(HOS) < μ(OHS). Interestingly, on the basis of η values HSO is predicted to be more stable than HOS in agreement with the prediction from the G-2 theory.[30] The HF method predicts the ^{3}A″ state of HSO^+ to be more stable than the ^{1}A′ state over the entire PE surface, which is not correct. Despite this gross deficiency, the HF method yields results in agreement with MHP, which is rather theoretically inconsistent.

Using a model diatomic molecule, Pal et al.[38] have recently shown that at constant chemical potential the finite difference approximation of hardness gives a maximum where the vertical ionization potential is maximum. This conclusion is found to be valid in the present systems also even though the chemical potential is not constant over the PE surface. The I and η profiles (both HF and DFT) of HSO−HOS and the corresponding profiles (HF) of the ^{1}A′ state of HNO−HON exhibit remarkable correspondence with regard to the position of extrema. The DFT I and η profiles of the latter show reasonable agreement when I and A are calculated using Koopmans' approximation.

D. Accurate Estimates of η and μ at the Stationary Points of the Energy Surfaces. Since the stationary points in the η and μ profiles are obtained only in qualitative correspondence with those in the respective PE curves, we have calculated these quantities at the B3LYP geometries. For this purpose the ionization potential and electron affinity are computed using PUMP2 (Full), PUMP4SDTQ (Full), and B3LYP methods. These computed values are given in Table 4. The ionization potential of HSO is calculated with respect to HSO^+(^{1}A′) and that of HOS refers to HOS^+(^{3}A″). The few experimental data that are available for comparison refer to the adiabatic values. In the case of the ^{1}A′ state of HNO all three methods predict[26] I_{ad} in good accord with experiment. The G-2 theory predicts a value of 10.27 eV, which is the same as the B3LYP adiabatic ionization potential. The G-2 estimate[26] for the ionization potential in the ^{3}A″ state of HON is 9.71 eV, which is in good agreement with the DF as well as MPn values. For the HSO radical MPn I values differ from experiment by a greater margin (∼0.6 eV) than the B3LYP value (the difference is about 0.4 eV). The ionization energy for the process HSO(^{2}A″) → HSO^+(^{3}A″) has been estimated[31] to be 11.15 eV. The B3LYP value is in very good accord with this experimental estimate. For both HSO and HOS the MRDCI values[29] of adiabatic ionization potential are underestimated by a margin of about 1.0 eV with respect to their DFT counterparts.

TABLE 4: Vertical (v) and Adiabatic (a) Ionization Energies (I, eV) and Electron Affinities (A, eV) of HNO−HON and HSO−HOS Systems

system XYZ	state	I v	I a	A v	A a	method[a]
HNO	^{1}A′	10.631	9.983	−0.392	0.082	A
		10.426	9.926	−0.481	0.180	B
		10.645	10.264	0.234	0.355	C
			10.100		0.338	exptl
HNO	^{3}A″	9.757	9.077	0.464	0.938	A
		9.563	9.063	0.382	0.881	B
		10.203	9.821	0.679	1.098	C
HON	^{1}A′	8.862	8.567	−0.951	0.468	A
		8.871	8.631	−1.120	0.362	B
		9.414	9.188	0.554	0.811	C
HON	^{3}A″	9.872	9.577	−1.961	−0.542	A
		9.751	9.510	−1.999	−0.516	B
		10.292	10.066	−0.323	−0.066	C
OHN	^{1}A′	10.117		−0.347		A
		9.989		−0.561		B
		10.053		0.940		C
OHN	^{3}A″	10.145		−0.797		A
		9.899		−0.730		B
		11.029		0.443		C
HSO[b]	^{2}A″	9.382	9.302	1.025	1.112	A
		9.402	9.353	0.886	1.003	B
		10.456	10.303	1.149	1.265	C
			9.340		2.590	D
				9.918		exptl
HOS[c]	^{2}A″	9.324	9.092	1.084	1.286	A
		9.281	9.105	0.061	1.293	B
		10.845	10.633	1.510	1.740	C
			9.670		1.970	D
OHS[d]	^{2}A″	9.225		2.007		A
		9.129		1.844		B
		10.149		1.667		C

[a] The calculated values shown against methods A, B, C, and D correspond respectively to PUMP2(Full)/X, PUMP4STQ (Full)/X, B3LYP/X, and MRDCI calculations,[29] where X = 6-311++G**. [b] With respect to HSO^+(^{3}A″) B3LYP, MRDCI, and experimental values[31] of I (adiabatic) are 11.034, 10.44, and 11.15 eV, respectively. [c] With respect to HOS^+ (^{1}A′) B3LYP and MRDCI values[29] of I (adiabatic) are 10.43 and 9.18 eV, respectively. [d] With respect to OHS^+ (^{3}A″).

The MPn and B3LYP electron affinity values are in satisfactory agreement for HNO and HSO. However, for HON and HOS, they differ by about 0.5 eV. It is difficult to offer a plausible explanation for this discrepancy. Tschumper and Schaefer[39] made an exhaustive comparative study of the performance of various versions of DFT in the calculation of electron affinity of small molecules. We could not identify any specific trend in the magnitude of errors in their calculated values. Sometimes they are obtained in very good accord with experiment, and in many cases they are overestimated by as much as 1.0 eV. For the HNO(^{1}A′) molecule the present calculations (B3LYP/6-311++G**) predict EA in excellent agreement with experiment, whereas the value obtained by Tschumper and Schaefer[39] using a better basis set differs from experiment by 0.4 eV. For the HSO radical the MRDCI value

TABLE 5: Hardness (η, eV) and Chemical Potential (μ, eV) of HNO−HON and HSO−HOS Systems at the Stationary Points in the Respective B3LYP PE Surface

		η^a			$-\mu^a$		
system	state	A	B	C	A	B	C
HNO	^{1}A′	5.503	5.545	5.206	5.111	4.973	5.441
HON	^{1}A′	4.907	4.99	4.430	3.956	3.876	4.984
OHN	^{1}A′	5.232	5.275	4.556	4.88	4.714	5.497
HNO	^{3}A″	4.647	4.591	4.762	5.111	4.973	5.441
HON	^{3}A″	5.917	5.875	5.308	3.956	3.876	4.984
OHN	^{3}A″	5.471	5.315	5.293	4.674	4.585	5.636
HSO	^{2}A″	4.179	4.258	4.654	5.204	5.144	5.803
HOS	^{2}A″	4.120	4.110	4.168	5.204	5.171	5.678
OHS	^{2}A″	3.608	3.643	4.241	5.616	5.487	5.908

[a] Values under columns A, B, and C correspond respectively to PUMP2(Full), PUMP4SDTQ (Full), and B3LYP calculations.

is overestimated by about 1.3 eV with respect to B3LYP value while for HOS the two methods yield comparable result.

The η and μ values obtained using the vertical I and A values of Table 4 are summarized in Table 5. On the basis of η values, the HNO radical in the ^{1}A′ state is predicted to be more stable than HON in the same state by both MPn and B3LYP calculations. In the ^{3}A″ state the MPn η values are in accord with the relative stability of HON and HNO. For the HSO−SOH system all three methods correctly predict HSO to be more stable than HOS on the basis of η. The ideal ordering, η(more stable isomer) > η(less stable isomer) > η(TS), is followed by the MPn methods only in the case of the ^{1}A′ state of HNO−HON. Kar and Scheiner[17] observed that μ like η is not a good indicator of the more stable isomer. The μ profiles of HNO−HON(^{1}A′) and HSO−HOS obtained here support this observation. However, the more accurate values of Table 5 do not follow any particular trend.

4. Concluding Remarks

The success of the B3LYP method in the calculation of electronic structure, relative energies, ionization potentials, and electron affinities of HNO−HON and HSO−HOS systems lends further support to the well-documented trend that this approach is quite reliable in the study of structure and energetics of a wide variety of molecules. So far this is the highest level of theory that has been employed in the calculation of η and μ profiles. Although the basis set used here is sufficiently extensive there is some room for improvement by extending it further. We have for the first time made a comparative study of HF and DFT methods to assess their performance in the calculation of η and μ profiles. The fact that HF and B3LYP methods give qualitatively similar results for these profiles may indicate that the former approach is adequate for this purpose. This is, however, not generally true since the HF method cannot always predict the correct ground state for the ions of open-shell species. Moreover, the UHF wave function usually contains a higher degree of spin contamination than a DODS (different orbitals for different spin) wave function based on KS orbitals. It has already been pointed out that the use of KA in the B3LYP method gives rise to quite unrealistic I and A values. Therefore, it is preferable to use the energy difference method in the density functional calculations of η and μ.

The maximum hardness principle[7] is strictly applicable to the change in a system when it evolves from one ground state to another. For the HNO−HON system neither the ^{1}A′ nor the ^{3}A″ PE curve represents a ground state over the entire reaction path, and the status of the two states is interchanged beyond their crossing point. The B3LYP method, although it yields a η profile of the ^{1}A′ state in qualitative agreement with MHP, fails to do so in the case of the ^{3}A″ state. This anomalous situation arises due to curve crossing and due to the nature of the variation of the difference in energies of the two states along the reaction path.

Finally, a few comments are necessary on the relative stability of the TS on the basis of η values. According to Pearson and Palke,[11] the TS in a reaction will have minimum hardness if it belongs to a different point group than both the reactant and the product. Such a situation occurs[11,17] in inversion, asymmetric deformation, internal rotation, and many isomerization reactions. In the present investigation HAB, HBA, and TS all belong to the same point group (C_s). Also, the extrema in the μ and E_{el} profiles do not coincide at the TS. So there is no rigorous reason for η to be minimum at the TS geometry.

Acknowledgment. A.B.S. is thankful to the Council of Scientific and Industrial Research, Government of India, for the award of Emeritus Scientistship and for financial support given to this work. He is also grateful to the Indian Institute of Technology, Kharagpur, for providing him with research facilities.

References and Notes

(1) Mulliken, R. S. *J. Am. Chem. Soc.* **1952**, *74*, 811.
(2) Pearson, R. G. *J. Am. Chem. Soc.* **1963**, *85*, 3533. Pearson, R. G. *Science* **1966**, *151*, 172.
(3) Parr, R. G.; Yang, W. *Density Functional Theory of Atoms and Molecules*; Oxford University Press: New York, 1989.
(4) Parr, R. G.; Pearson, R. G. *J. Am. Chem. Soc.* **1983**, *105*, 7512.
(5) Parr, R. G.; Donnelly, R. A.; Levy M.; Palke, W. E. *J. Chem. Phys.* **1978**, *69*, 4431.
(6) Pearson, R. G. *Proc. Natl. Acad. Sci. U.S.A.* **1985**, *82*, 6723.
(7) Pearson, R. G. *J. Chem. Educ.* **1987**, *64*, 561. Parr, R. G.; Chattaraj, P. K. *J. Am. Chem. Soc.* **1991**, *113*, 1854. Pearson, R. G. *Acc. Chem. Res.* **1993**, *26*, 250.
(8) Parr, R. G.; Gazquez, J. L. *J. Phys. Chem.* **1993**, *97*, 3939. Gazquez, J. L.; Martinez, A.; Mendez, F. *J. Phys. Chem.* **1993**, *97*, 4059.
(9) Galvan, M.; Pino, A. D., Jr.; Joannopoulos, J. D. *Phys. Rev. Lett.* **1993**, *70*, 21. Pino, A. D., Jr.; Galvan, M.; Arias, T. A.; Jannopoulos, J. D. *J. Chem. Phys*. **1993**, *98*, 1606.
(10) Datta, D. *J. Phys. Chem.* **1992**, *96*, 2409. Datta, D. *Inorg. Chem.* **1992**, *31*, 2797. Hati, S.; Datta, D. *J. Phys. Chem.* **1994**, *98*, 10451; **1995**, *99*, 10742.
(11) Pearson, R. G.; Palke, W. E. *J. Phys. Chem.* **1992**, *96*, 3283. Chattaraj, P. K.; Nath, S.; Sannigrahi, A. B. *Chem. Phys. Lett.* **1993**, *212*, 223. Pal, S.; Naval, N.; Roy, S. *J. Phys. Chem.* **1993**, *97*, 4404.
(12) Mendez. F.; Gazquez, J. L. *J. Am. Chem. Soc.* **1994**, *116*, 9298. Mendez, F.; Gazquez, J. L. *Proc. Ind. Acad. Sci. (Chem. Sci.)* **1994**, *106*, 183.
(13) Cardens-Jiron, G. I.; Torro-Lobe, A. *J. Phys. Chem.* **1995**, *99*, 12730.
(14) Roy, R. K.; Chandra, A. K.; Pal, S. *J. Phys. Chem.* **1994**, *98*, 10447. Pal, S.; Chandra, A. K. *J. Phys. Chem.* **1995**, *99*, 13865. Pal, S.; Chandra, A. K.; Roy, R. K. *J. Mol. Struct. (THEOCHEM)* **1996**, *361*, 57.
(15) Nath, S.; Sannigrahi, A. B.; Chattaraj, P. K. *J. Mol. Struct. (THEOCHEM)*, **1994**, *309*, 65. Sannigrahi, A. B.; Nandi, P. K. *J. Mol. Struct. (THEOCHEM)* **1994**, *307*, 99.
(16) Chattaraj, P. K.; Nath, S.; Sannigrahi, A. B. *J. Phys. Chem.* **1994**, *98*, 9143.
(17) Kar, T.; Scheiner, S. *J. Phys. Chem.* **1995**, *99*, 8121. Ghanty, T. K.; Ghosh, S. K. *J. Phys. Chem.* **1996**, *100*, 2295.
(18) De Proft. F.; Langenaeker, W.; Geerlings, P. *J. Phys. Chem.* **1993**, *97*, 1826. Roy, R. K.; Pal, S. *J. Phys. Chem.* **1995**, *99*, 17822. Kar, T.; Scheiner, S.; Sannigrahi, A. B. *J. Mol. Struct. (THEOCHEM)* **1998**, *427*, 79.
(19) Kohn, W.; Sham, L. J. *Phys. Rev.* **1965**, *A140*, 1133.
(20) Becke, A. D. *J. Chem. Phys.* **1992**, *96*, 2155; **1993**, *98*, 5648.
(21) Lee, H.; Yang, W.; Parr, R. G. *Phys. Rev.* **1988**, *B37*, 785.
(22) Cui, Q.; Musaev, D. G.; Svenson, M.; Sieber, S.; Morokuma, K. *J. Am. Chem. Soc.* **1995**, *117*, 12366. Ricca, A.; Bauschlicher, C. W. *J. Phys. Chem.* **1995**, *97*, 5922, 9003. Jemmis, E. D.; Subramanian, G.; Korkin, A. A.; Hofmann, M.; Schleyer, P. v. R. *J. Phys. Chem. A* **1997**, *101*, 919.
(23) Frisch, M. J.; Trucks, G. W.; Schlegel, H. B.; Gill, P. M. W.; Johnson. B. G.; Robb, M. A.; Cheeseman, J. R., Keith, T.; Petersson, G. A.; Montgomery, J. A.; Raghavachari, K.; Al− Laham, M. A.; Zakrzewski,

V. G.; Ortiz, J. V.; Foresman, J. B.; Cioslowski, J.; Stefanov, B. B.; Nanayakkara, A.; Challacombe, M.; Peng, C. Y.; Ayala, P. Y.; Chen, W.; Wong, M. W.; Andres, J. L.; Replogle, E. S.; Gomperts, R.; Martin, R. L.; Fox, D. J.; Binkley, J. S.; Defrees, D. J.; Baker, J.; Stewart, J. P.; Head-Gordon, M.; Gonzalez, C.; Pople, J. A. Gaussian-94 (Revision E), Gaussian Inc. Pittsburgh, PA, 1995.

(24) Sengupta D.; Chandra, A. K. *J. Chem. Phys.* **1994**, *101*, 3906 and references therein.

(25) Guadagnini, R.; Schatz, G. C.; Walch, S. P. *J. Chem. Phys*. **1995**, *102*, 774 and references therein. Experimental values of geometry quoted in this paper have been used here for comparison.

(26) Mebel, A. M.; Luna, L.; Morokuma, K. *J. Chem. Phys*. **1996**, *105*, 31807.

(27) Luke, B. T.; McLean, A. D. *J. Chem. Phys.* **1985**, *89*, 4592.

(28) Meier, U.; Staatsexamensarbeit, Bonn University, 1984.

(29) Bruna, P. J.; Peyerimhoff, S. D. In *Ab initio Methods in Quantum Chemistry*; Lawley, K. P., Ed.; John-Wiley: New York, 1987; Part I, p 1.

(30) Goumri, A.; Laakso, D.; Rocha, J.-D. R.; Smith, C. E.; Marshall, P. *J. Chem. Phys.* **1995**, *102*, 161 and references therein.

(31) Cheng, B. M.; Ebberhard, J.; Chem. W-C.; Yu, C-h. *J. Chem. Phys.* **1997**, *106*, 9727.

(32) Ohashi, M.; Kakimoto, M.; Saito, S.; Hirota, E. *J. Mol. Spectrosc*. **1980**, *84*, 204.

(33) Sannigrahi, A. B.; Thunemann, K. H.; Peyerimhoff, S. D.; Buenker, R. *J. Chem. Phys.* **1977**, *20*, 25. Sannigrahi, A. B.; Peyerimhoff, S. D.; Buenker, R. *J. Chem. Phys*. **1977**, *20*, 381. Buenker, R. J.; Bruna, P. J.; Peyerimhoff, S. D. *Isr. J. Chem*. **1980**, *19*, 309.

(34) A comprehensive list of earlier ab initio calculations on HSO−SOH is included in ref 30.

(35) Xantheas, S. S.; Dunning Jr., T. H. *J. Phys. Chem.* **1993**, *97*, 6616. Essefar, M.; Mo, O.; Yanez, M. *J. Chem. Phys.* **1994**, *101*, 2175.

(36) Curtiss, L. A.; Raghavachari, K.; Trucks, C. W.; Pople, J. A. *J. Chem. Phys*. **1991**, *94*, 7221.

(37) The $^3A''$ and $^1A'$ μ profiles are exactly identical since *I* and *A* are calculated at the same geometry using same energies for A^+ or A^- for both the states. In fact, it can be shown in a straightforward manner that under aforementioned conditions, $2\mu = E^- - E^+$ for any electronic state of a molecule (A).

(38) Pal, S.; Roy, R. K.; Chandra, A. K. *J. Phys. Chem.* **1994**, *98*, 2314.

(39) Tschumper, G. S.; Schaefer III, H. F. *J. Chem. Phys.* **1997**, *107*, 2529.